

## Out of plane behavior of walls, using rigid block concepts

Mohammadi Gh.M.<sup>†</sup> and Yasrebi F.<sup>‡</sup>

*International Institute of Earthquake Engineering and Seismology (IIEES),  
No. 21, Arghavan gharbi, Dibaji shomali, Dr. Lavasani St., Tehran, I.R. Iran*

*(Received February 12, 2008, Accepted November 9, 2009)*

**Abstract.** Out of plane behaviors of walls and infills are investigated in this paper, using rigid block concepts. Walls and infills are sometimes separated from top beams because of in plane movement of the walls and crumbling mortar layers under the top beams. Therefore, sufficient strength should be supplied to hold them against out of plane forces. Such walls are studied here under some real and scaled earthquakes, regarding their out of plane behavior. Influences of some reinforcements, connecting the walls to frames or perpendicular walls, are also studied. It is shown that unreinforced walls of regular sizes (3 m high and 4.5 m long) are normally unstable in the earthquakes. However, performing some reinforced bars that connect them to adjacent elements- frames or perpendicular walls - stabilizes them. Eventually, it is concluded that supplying 3 reinforced bars at 1/4, 2/4 and 3/4 of the panel's height stabilizes the walls in the assumed earthquakes. In this regard, for 20 cm and 35 cm thick walls  $\Phi 18$ mm and  $\Phi 20$ mm bars are to be used, respectively. For walls with other configurations, the forces and required areas of the reinforcements can be determined by the developed method of this paper.

**Keywords:** rigid block; wall; infill; out of plane; seismic behavior; reinforcement.

---

### 1. Introduction

Out of plane strength of walls affects structural behavior and earthquake mitigation. Therefore, the out-of-plane strength of walls should be checked and enough out of plane resistance be supplied against seismic loads (De Felice *et al.* 2001).

Top bricks layer inclining of about  $45^\circ$  sometimes improve the gap, but still do not supply enough connection. On the other hand, X pattern of cracks, resulting from in-plane forces, is similar to the crack pattern for a square panel subjected to out-of-plane forces. This implies that the transverse strength can be substantially weakened by in-plane cracking. Therefore, out-of-plane strength of a cracked infill is often surmised to be quite low (Angle *et al.* 1994). In this regard, Mendola *et al.* (1995) translated the problem into the analysis of a fixed-free ended prismatic column, undergoing static horizontal forces equivalent to the maximum inertia actions.

To study the effects of transversal earthquake on the masonry infilled frames behavior, Flanagan *et al.* (1994) performed a lot of tests, in which the specimens were loaded in two transversal

---

<sup>†</sup> Assistant Professor, Corresponding author, E-mail: [ghazimahalleh@gmail.com](mailto:ghazimahalleh@gmail.com)

<sup>‡</sup> MSc

directions. The results showed that the specimens subjected to cyclic out of plane drift displacement were stable, within the range a typical infill might experience. For such specimens, only minimal degradation of in-plane stiffness and strength would happen if they are loaded in plain. Some other infill panels were tested using sequential in-plane and out-of-plane pressure. They showed zero to 15% reduction in out-of-plane capacity, after being initially loaded by 75% of ultimate in-plane strength. Alternatively, another specimen was simultaneously loaded by in-plane and out-of-plane forces, showing no significant interaction at low to moderate loading levels.

A shaking table test with bidirectional excitation on two-story, square in plan, concrete frame structure, showed that infill panels by a clear height of 2.5 m and the thickness of 11.5 or 8.0 cm would sustain lateral accelerations of about 1.75 g or 1.3 g, respectively, showing no out of plane expulsion or significant damage (Fardis *et al.* 1999). Nevertheless, unreinforced masonry (URM) infill walls have demonstrated poor performance records even in moderate earthquakes and they need to be strengthened. Adding new structural frames or shear walls, is impractical due to its cost or its restriction in being used in certain types of structures. Therefore, other strengthening methods, such as: grout injection, insertion of reinforcing steel, pre-stressing, jacketing and using polymer laminates (FRP<sup>1</sup>) were proposed by El-Dakhkhni (2006).

The arching action, a source of infill out of plane resistance, depends on the infill material, twisting stiffness of frame members and the infill to frame connection status. The gaps are developed at the top of the walls soon after being constructed, due to the mortar shrinkage. The walls, with top gaps, cannot withstand the out-of-plane forces in the earthquakes and would collapse due to the inadequate binding at the top. However, the walls surrounded by rigid supports, can display high resistance to out-of-plane forces for the development of arching action in flexure. Therefore, to achieve an optimal load-bearing behavior- or rather stability, the remaining gaps at the top of the walls are recommended to be filled with non-shrinkable mortar some days after their construction (Dafnis *et al.* 2002).

The first author believes that out of plane strength of a masonry infill is overestimated by the proposed formulas, e.g., the Angel formula- Proposed in FEMA-273 (1997) and FEMA-356 (2000) - or experimented in the above-mentioned bidirectional excitation. Because they ignore the worst case, in which the transversal acceleration occurs where the wall has experienced interface cracking but returns back to its normal position (zero drift). In such a case, integration between infill and frame is minimum. Therefore, it is highly suggested to ignore the arching action and supply the required out of plane resistance by reinforced bars or mesh.

The out-of-plane behavior of masonry walls is studied in this research, assuming walls as rigid blocks, disregarding their curvature. For the purpose, governing formula are derived and solved for a rigid block under Manjil, Bam, Taft, Tabas, Tarzana, Kobe and Elcentro earthquake records. For each earthquake, two cases- natural records and normalized to 0.5 g - are considered (g is ground natural acceleration). The walls curvature for the lateral loads can disregarded for thick concrete walls or infills, yet it is not as much erroneous for concrete or even masonry infills of normal thicknesses.

The calculation is based on the equation of a rigid body motion, freely oscillates and topples on rigid or flexible foundations. This has been studied for many years; in 1963, a rigid block problem was analyzed by Housner (1963) which was developed by Makris *et al.* (2000) for sinusoidal excitation (Zang *et al.* 2001). The analytical free motion problem for small rotations and sinusoidal

---

<sup>1</sup>Fiber Reinforced Polymer

excitation is analyzed by Yim *et al.* (1980).

Here, the behavior of walls or infills with top gaps is investigated against out of plane earthquake loads. In this regard, some reinforced bars are applied at 1/4, 2/4 and 3/4 of the walls height. The iterative procedure using rigid block concepts is performed for the analysis. Two masonry walls with two different thicknesses, 20 or 35 cm, are considered here. It is assumed that the length and height of the walls are 4.5 and 3 m, respectively, made by a 18 kN/m<sup>3</sup> dense masonry material.

### 2. Analysis procedure

A developed MATLAB code (2006) is utilized for the analysis, on the adopted mathematical model, which is briefly reviewed as follows:

The formula of motion is written for a rigid block by the length, height and thickness of  $l$ ,  $h$  and  $t$ , respectively, shown in Fig. 1, as

$$x = R[\sin \theta_c - \sin(\theta_c - |\theta|)] \tag{1}$$

and

$$y = R[\cos(\theta_c - |\theta|) - \cos \theta_c] \tag{2}$$

where  $x$  and  $y$  are horizontal and vertical displacements of gravity center of the block, respectively, and

$$R = 0.5 \times \sqrt{t^2 + h^2} \tag{3}$$

$\theta$  is the block rotation angle,  $|\theta|$  is the absolute value of block rotation angle.  $\theta_c$  is the critical rotation angle, calculated by

$$\theta_c = \arctan(t/h) \tag{4}$$

The accelerations of the block gravity center in horizontal and vertical directions are obtained by second order derivatives of formulas 1 and 2, as below

$$\ddot{x} = \pm R \ddot{\theta} \cos(\theta_c - |\theta|) + R \dot{\theta}^2 \sin(\theta_c - |\theta|) \tag{5}$$

and

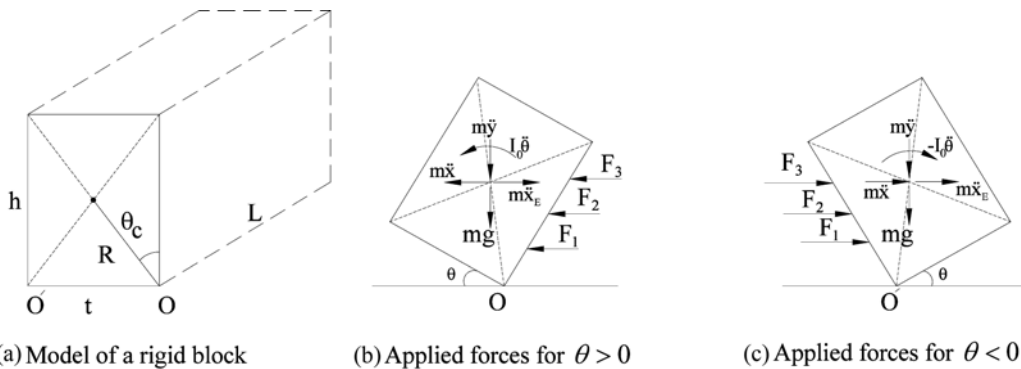


Fig. 1 Models and the applied forces on a rigid block

$$\ddot{y} = \pm R \ddot{\theta} \sin(\theta_c - |\theta|) - R \dot{\theta}^2 \cos(\theta_c - |\theta|) \tag{6}$$

where, the positive and negative signs (regarding the coupled ones) refer to the cases of  $\theta > 0$  and  $\theta < 0$ , respectively.

Based on equilibrium relations, the summation of all applied moments around point O is zero, therefore

$$I \ddot{\theta} + mgR \cos\left(\frac{\pi}{2} - \theta_c + \theta\right) + m \ddot{x}_E R \sin\left(\frac{\pi}{2} - \theta_c + \theta\right) + m \ddot{y} R \cos\left(\frac{\pi}{2} - \theta_c + \theta\right) = m \ddot{x}_E R \sin\left(\frac{\pi}{2} - \theta_c + \theta\right) \tag{7}$$

where,  $\ddot{x}_E$  is the horizontal acceleration of earthquake perpendicular to the wall surface,  $m$  is mass of the block and  $g$  is natural ground acceleration.

Substituting  $\ddot{x}$  and  $\ddot{y}$  of formulas 5 and 6 into relation 7 gives the following relation (illustrated more by Jeong *et al.* 1997)

$$\ddot{\theta} \pm \omega^2 \left[ \sin(\theta_c - |\theta|) \mp \frac{\ddot{x}_E(t)}{g} \cos(\theta_c - |\theta|) \right] = 0 \tag{8}$$

where, in case of applying the top and bottom signs (regarding the coupled plus minus), the formula refer to  $\theta > 0$  and  $\theta < 0$ , respectively, and

$$\omega^2 = \frac{3g}{4R} \tag{9}$$

It can be assumed that for small rotation angles  $\theta = \sin(\theta)$ ; therefore, block period of free vibration can be calculated as

$$T = 2\pi / \left( \sqrt{\frac{3g}{4R} \times \left( \cos \theta_c + \frac{\ddot{x}_E}{g} \sin \theta_c \right)} \right) \tag{10}$$

Since  $\theta_c$  is a very small angle ( $3.81^\circ$  and  $6.65^\circ$  for the 0.2 and 0.35 m thick wall), the influence of the term  $\ddot{x}_E/g$  on the period is negligible.

Each reinforced bar is considered as a spring by the stiffness of  $k$ , composed of two parts,  $k_b$  and  $k_a$ , regarding the bending and axial stiffness of bars, respectively. Deformation of a bar and wall, caused by vibration of the wall, is shown in Fig. 2(a).

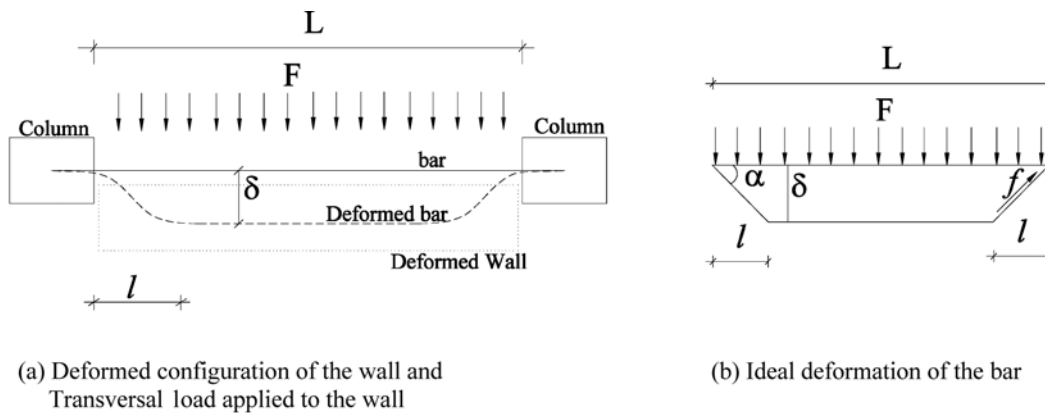


Fig. 2 Deformed configuration of the wall and reinforcement

During an earthquake, bars and mortar are separated. In the corners, the mortar is crumbled and put out of the joint in the area of  $l$  length. In these parts the bar can oscillate freely; however, they remain attached in the other parts.

Bending stiffness of the bar,  $k_b$ , can be calculated as follows, regarding the its deformed shape shown in Fig. 2(b)

$$k_b = 72EI/(L \times l^2) \quad (11)$$

where,  $E$  and  $I$  are elasticity modulus and the second moment of area of the bar, respectively.

Lateral displacement of reinforced bar ( $\delta$ ), shown in Fig. 2(b), is

$$\delta = l \times \tan \alpha \quad (12)$$

where  $\alpha$  is shown in Fig. 2(b).

Assuming a uniform load ( $F$ ) on the wall, caused by transversal earthquake component, gives the bar axial load ( $f$ ) as

$$f = F/(2 \sin \alpha) \quad (13)$$

Regarding that the bar has almost constant axial force of  $f$ , its elongation is

$$\Delta l = (f \times L)/(A \times E) = FL/(2AE \sin \alpha) \quad (14)$$

where,  $A$  and  $E$  are area and elasticity modulus of the bar, respectively.

Based on the geometry of the deformed configuration, Fig. 2(b),  $\Delta l$  is

$$\Delta l = 2(l/\cos \alpha - l) = 2l(1/\cos \alpha - 1) \quad (15)$$

The force  $F$  can be determined by omitting  $\Delta l$  from Eqs. (14) and (15), as

$$F = 4EA \times \tan(\alpha) \times (1 - \cos(\alpha)) \times \frac{l}{L} \quad (16)$$

Axial stiffness of the bars,  $k_a$ , can be calculated as follows, regarding relations 12 and 16

$$k_a = F/\delta = 4EA(1 - \cos \alpha)/L \quad (17)$$

Therefore, entire stiffness of a bar against block rigid body motion is

$$k = k_b + k_a = \frac{72EI}{L \times l^2} + \frac{4EA}{L}(1 - \cos \alpha) \quad (18)$$

$k$ ,  $k_b$  and  $k_a$  are calculated and shown in Fig. 3 for a 20 cm thick walls, assuming  $l = 20$  cm:  $k_b$  is constant but  $k_a$  rises by increasing the amplitude of vibration ( $\delta$ ). For normal  $\delta$ , both  $k_a$  and  $k_b$  should be considered in the analysis.

Formula 8 will be improved as follows, regarding the effects of reinforced bars as shown in Fig. 4

$$\ddot{\theta} \pm \omega^2 \left[ \sin(\theta_c - |\theta|) \mp \left( \frac{\ddot{x}_F}{g} \right) \cos(\theta_c - |\theta|) \right] \pm \left( \frac{3}{4mR^2} \right) \sin|\theta| \times \sum k_i h_i^2 = 0 \quad (19)$$

where,  $k_i$  is the entire stiffness of  $i^{\text{th}}$  reinforced bar (including  $k_a$  and  $k_b$ ) connected to the block at the height of  $h_i$ . In this relation, similar to formula 8, the top and bottom signs (concerning coupled plus/minus) refer to the cases where  $\theta > 0$  and  $\theta < 0$ , respectively.

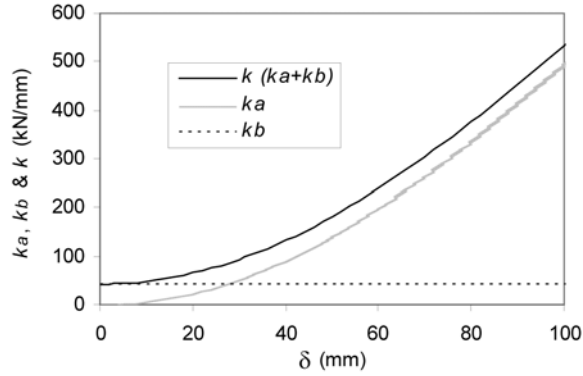


Fig. 3 Comparing  $k$ ,  $k_a$  and  $k_b$

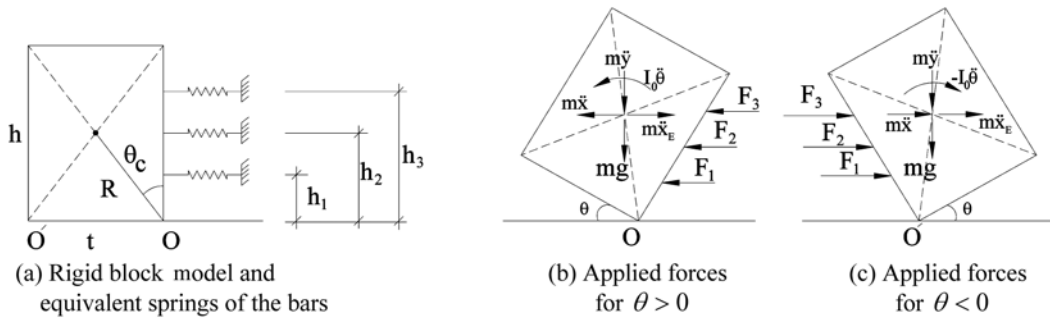


Fig. 4 Models and the applied forces on a reinforced wall, considered as a rigid block

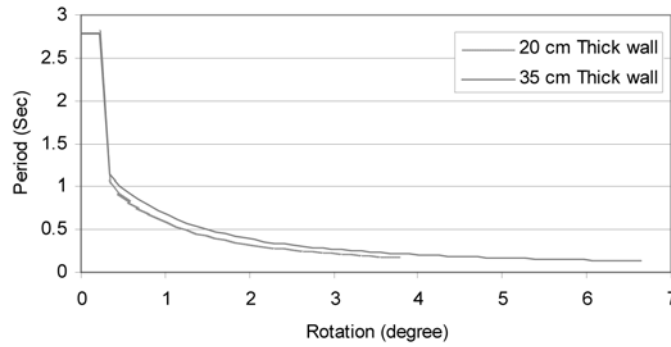


Fig. 5 Relation between natural vibration period and rotation angle for the 20 and 35 cm thick walls

The block period of free vibration, for small rotation angles ( $\theta$ ), can be calculated as

$$T = 2\pi / \left( \sqrt{\frac{3g}{4R} \times \left( \cos \theta_c + \frac{\ddot{x}_E}{g} \sin \theta_c \right) - \frac{3}{4mR^2} \sum (h_i^2 \times k_i)} \right) \quad (20)$$

Relations between the natural vibration period ( $T$ ) and the rotation angle ( $\theta$ ) are shown in Fig. 5, for the 20 cm and 35 cm thick walls. It is assumed here that  $l=10$  cm and the walls have 3 horizontal reinforced bars of  $\Phi 18$  and  $\Phi 20$ , respectively, equally spaced at the middle half of the wall.

### 3. Solving the equations

Eq. (19) is solved by iterative methods, based on the Taylor expansion equation as follows

$$\theta_{i+1} = \theta_i + \Delta t \cdot \dot{\theta}_i + (\Delta t)^2/2 \ddot{\theta}_i + (\Delta t)^3/6 \theta_i^{(III)} + (\Delta t)^4/24 \theta_i^{(IV)} \quad (21)$$

In order to minimize the errors, enough discretization of acceleration records is performed, similar to other time history analyses. In which linear relationship between time and acceleration is assumed in every time step. The calculation starts by the assumption of  $\dot{\theta}_0 = 0$ .

To consider the impact mechanisms, Housner (1963) assumed a restitution coefficient,  $\beta$ , that multiplies the angular velocity  $\dot{\theta}$  if the block passes through the equilibrium position at  $\theta = 0$ . Considering the existence of angular moment conservation before and after an impact, the restitution coefficient can be obtained through

$$\beta = \frac{\dot{\theta}^+}{\dot{\theta}^-} = 1 - \frac{3}{2} \sin^2 \theta \quad (22)$$

where,  $\dot{\theta}^-$  and  $\dot{\theta}^+$  are the angular velocities just before and after the impact, respectively (Pena *et al.* 2007).

### 4. Analysis results

Two walls of 20 and 35 cm thick, by the height and length of 3 and 4.5 m respectively, are investigated. 7 earthquake records, including Taft, Manjil, Bam, Tabas, Tarzana, Elcentro and Kobe are considered. PGAs<sup>1</sup> of these records are 0.5806 g, 0.5506 g, 0.5000 g, 0.4551 g, 0.4489 g, 0.4420 g and 0.3757 g, respectively (g is the natural ground acceleration). The spectra of the above mentioned earthquakes, normalized to 1.0 g, are shown in Fig. 6.

A time-history analysis has been done for each earthquake record. Results of the 20 cm wall for Taft earthquake is shown in Fig. 7, in which the earthquake acceleration, wall rotation angle ( $\theta$ ), as well as the tensile forces of the bottom, middle and top reinforced bars (F1, F2 and F3,

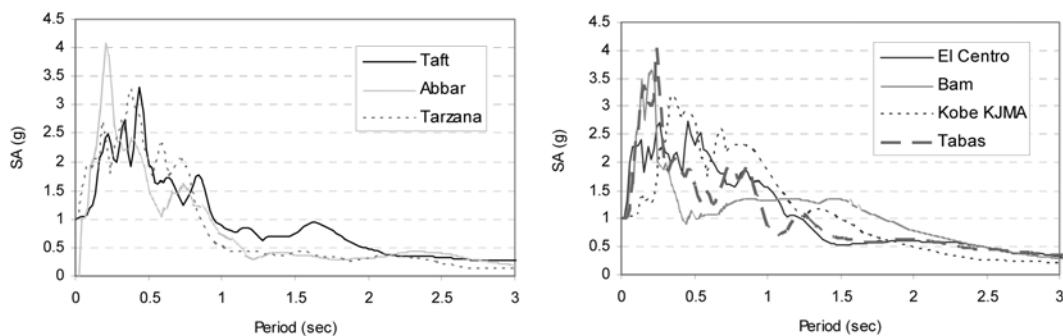


Fig. 6 Spectra of Taft, Manjil, Bam, Tabas, Tarzana, Elcentro and Kobe earthquakes

<sup>1</sup>Peak Ground Acceleration

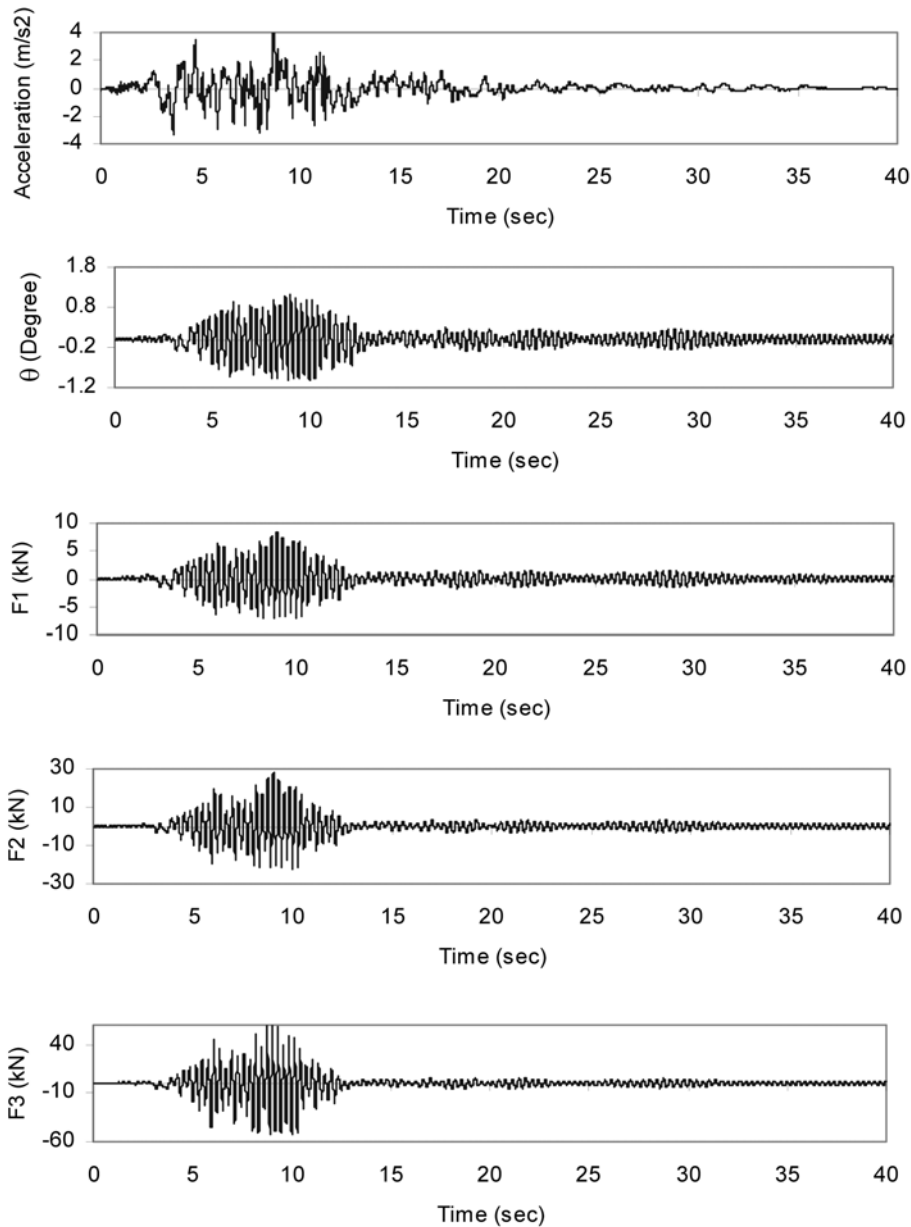


Fig. 7 Time history of the horizontal ground acceleration, wall rotation and reinforced bars' forces (F1, F2 and F3) in Taft earthquake for a 20 cm thick wall, assuming  $l = 20$  cm

respectively) are shown with respect to the time. Both negative and positive bar forces are tensile, however the negative ones are related to the negative wall rotations.

The results of time-history analyses of the 20 cm thick wall under real records of Taft, Manjil, Bam, Tabas, Tarzana, Elcentro and Kobe are summarized in Table 1. This table shows the PGA, the maximum block rotation in positive and negative directions ( $\theta^+$  and  $\theta^-$ , respectively), and the maximum tensile forces of the reinforcements (F1, F2 and F3), which connect the wall to the

Table 1 Results for a 20 cm thick wall in earthquakes of natural PGAs, assuming  $l = 20$  cm

Real Earthquake	PGA (g)	$\theta^+$ (deg)	$\theta^-$ (deg)	$F_3^+$ (kN)	$F_3^-$ (kN)	$F_2^+$ (kN)	$F_2^-$ (kN)	$F_1^+$ (kN)	$F_1^-$ (kN)
<b>TAFT</b>	<b>0.5806</b>	<b>1.13</b>	<b>1.19</b>	<b>69.97</b>	<b>-78.25</b>	<b>28.18</b>	<b>-31.05</b>	<b>8.37</b>	<b>-8.96</b>
MANJIL	0.5506	0.96	0.85	47.66	-36.00	20.32	-16.09	6.64	-5.62
BAM	0.5000	0.81	0.79	32.62	-30.61	14.83	-14.08	5.31	-5.11
TABAS	0.4551	0.68	0.66	22.78	-21.19	11.06	-10.43	4.27	-4.01
TARZANA	0.4489	1.13	1.01	68.53	-52.94	27.68	-22.20	8.26	-7.07
ELCENTRO	0.4420	1.00	1.00	52.29	-52.49	21.97	-22.04	7.02	-7.04
KOBE	0.3757	0.93	0.81	43.84	-32.25	18.95	-14.69	6.32	-5.27

Table 2 Results for a 20 cm thick wall in earthquakes PGA of 0.5 g, assuming  $l = 20$  cm

Scaled Earthquake	$\theta^+$ (deg)	$\theta^-$ (deg)	$F_3^+$ (kN)	$F_3^-$ (kN)	$F_2^+$ (kN)	$F_2^-$ (kN)	$F_1^+$ (kN)	$F_1^-$ (kN)
TAFT	0.96	0.92	47.53	-42.69	20.27	-18.53	6.63	-6.22
MANJIL	0.93	0.86	43.67	-36.93	18.89	-16.43	6.31	-5.71
BAM	0.81	0.79	32.62	-30.61	14.83	-14.08	5.31	-5.11
TABAS	0.71	0.75	24.50	-27.49	11.74	-12.89	4.47	-4.79
<b>TARZANA</b>	<b>1.32</b>	<b>1.21</b>	<b>101.46</b>	<b>-81.11</b>	<b>39.02</b>	<b>-32.04</b>	<b>10.54</b>	<b>-9.16</b>
ELCENTRO	1.03	1.03	55.66	-56.05	23.17	-23.30	7.29	-7.32
KOBE	0.99	0.92	50.25	-42.95	21.25	-18.62	6.86	-6.24

column at 1/4, 2/4 and 3/4 of the heights. Superscripts + or - corresponds to positive and negative rotation of wall, respectively. In this table, PGA, rotation and forces are in g, degree and kN, respectively. In these analyses the bars are assumed  $\Phi 18$ mm.

As shown in Table 1, Taft will produce the maximum wall rotation and bar forces. For each earthquake record, higher bar has greater tensile force,  $F_3 > F_2 > F_1$ .

For normalized records (to PGA of 0.5 g), the analyses led to different results, shown in Table 2: Tarzana produced the most critical case, in which the tensile force of the bar exceeded 101 kN.

Similarly, the behavior of a 35 cm thick wall is investigated under the earthquakes, for both natural record and normalized one (to 0.5 g). The results are presented in Table 3 and 4, respectively. In these analyses it is assumed that the wall has 3 bars of  $\Phi 20$ mm, at 1/4, 2/4 and 3/4 of the wall height and  $l = 20$  cm.

As it can be seen, for natural and normalized earthquake records, Taft and Elcentro produced the most critical cases, respectively, with the maximum reinforcement tensile forces of 117.28 and 115.70 kN, respectively.

In summary, for the records of natural PGA, Taft produces the most critical conditions, with maximum bar tensile forces of 78.25 and 117.28 kN in the 20 and 35 cm thick wall, respectively. However for normalized records, Tarzana and Elcentro are more dangerous, producing the maximum bar tensile forces of 101.46 and 124.70 kN in the 20 and 35 cm thick wall, respectively.

Table 3 Results for a 35 cm thick wall in earthquakes of natural PGA, assuming  $l = 20$  cm

Real Earthquake	PGA/g	$\theta^+$ (deg)	$\theta^-$ (deg)	$F_3^+$ (kN)	$F_3^-$ (kN)	$F_2^+$ (kN)	$F_2^-$ (kN)	$F_1^+$ (kN)	$F_1^-$ (kN)
<b>TAFT</b>	<b>0.5806</b>	<b>1.26</b>	<b>-1.14</b>	<b>117.28</b>	<b>-93.31</b>	<b>47.45</b>	<b>-38.99</b>	<b>14.13</b>	<b>-12.30</b>
Manjil	0.5506	1.24	-1.23	113.65	-110.94	46.18	-45.22	13.86	-13.66
BAM	0.5000	0.98	-1.07	66.12	-80.75	34.50	-14.08	10.01	-11.28
TABAS	0.4551	0.68	-0.69	31.43	-32.05	15.87	-16.12	6.39	-6.47
TARZANA	0.4489	1.07	-1.05	79.59	-77.16	34.08	-33.20	11.18	-10.98
ELCENTRO	0.4420	1.00	-1.00	69.20	-74.30	30.30	-32.2	10.30	-10.70
KOBE	0.3757	1.06	-1.04	78.15	-75.88	33.56	-32.74	11.06	-10.87

Table 4 Results for a 35 cm thick wall in earthquakes of normalized PGA, assuming  $l = 20$  cm

Scaled Earthquake	$\theta^+$ (deg)	$\theta^-$ (deg)	$F_3^+$ (kN)	$F_3^-$ (kN)	$F_2^+$ (kN)	$F_2^-$ (kN)	$F_1^+$ (kN)	$F_1^-$ (kN)
TAFT	1.07	-1.07	80.84	-80.73	34.53	-34.49	11.29	-11.28
Manjil	1.07	-1.14	81.39	-93.35	34.73	-39.00	11.33	-12.30
BAM	0.98	-1.07	66.12	-80.75	29.18	-34.50	10.01	-8.15
TABAS	0.83	-0.83	45.80	-46.77	21.57	-21.94	8.05	-8.15
TARZANA	1.26	-1.30	118.01	-127.60	47.70	-51.06	14.19	-14.89
<b>ELCENTRO</b>	<b>1.30</b>	<b>-1.30</b>	<b>124.70</b>	<b>-115.70</b>	<b>50.00</b>	<b>-46.90</b>	<b>14.70</b>	<b>-14.00</b>
KOBE	1.17	-1.07	99.47	-79.70	41.18	-34.12	12.78	-11.19

## 5. Effect of reinforcement yielding

In this part, the analysis is improved by considering the possibility of yielding for the reinforcement, which was ignored in previous parts.

The results show that for a 35 cm thick wall, maximum wall rotation rises from  $1.26^\circ$  to  $1.58^\circ$  for Taft and from  $1.24^\circ$  to  $1.25^\circ$  for Manjil record, Table 5, by regarding the yielding possibility of reinforced bars. For both of Taft and Manjil records, the maximum bar forces will be equal to the bar tensile strength, 94.25 kN, assuming that  $F_y = 300$  MPa ( $F_y$  is the yielding stress of reinforcement). For other records, the bar forces do not exceed yielding and the same results of Table 3 will be determined again.

Time-history of wall rotation angle in Taft earthquake, with and without considering bar yielding is shown in Fig. 8 as "Considering Yielding" and "Ignoring Yielding", respectively. According to the figure, wall rotation rises if the yielding is considered.

The results show that 20 cm thick walls can be stabilized against out of plane movement, by supplying three bars of  $\Phi 18$ mm. The bars connect the wall to the adjacent elements or perpendicular walls and are equally spaced at the middle half of the wall. For 35 cm thick walls,  $\Phi 20$ mm bars should be used instead. In case of necessity the reinforcement can be replaced by equivalent bars with the same stiffness.

Table 5 Results for a 35 cm thick wall in earthquakes of natural PGA, regarding yielding possibility of bars and assuming  $l = 20$

Real Earthquake	PGA/g	$\theta^+$ (deg)	$\theta^-$ (deg)	$F_3^+$ (kN)	$F_3^-$ (kN)	$F_2^+$ (kN)	$F_2^-$ (kN)	$F_1^+$ (kN)	$F_1^-$ (kN)
<b>TAFT</b>	<b>0.5806</b>	<b>1.49</b>	<b>-1.58</b>	<b>94.25</b>	<b>-94.25</b>	<b>67.7</b>	<b>-77.82</b>	<b>18.20</b>	<b>-20.13</b>
<b>Manjil</b>	<b>0.5506</b>	<b>1.25</b>	<b>-1.15</b>	<b>94.25</b>	<b>-94.25</b>	<b>46.74</b>	<b>-39.45</b>	<b>13.98</b>	<b>-12.40</b>
BAM	0.5000	0.98	-1.07	66.12	-80.75	34.50	-14.08	10.01	-11.28
TABAS	0.4551	0.68	-0.69	31.43	-32.05	15.87	-16.12	6.39	-6.47
TARZANA	0.4489	1.07	-1.05	79.59	-77.16	34.08	-33.20	11.18	-10.98
ELCENTRO	0.4420	1.00	-1.00	69.20	-74.30	30.30	-32.2	10.30	-10.70
KOBE	0.3757	1.06	-1.04	78.15	-75.88	33.56	-32.74	11.06	-10.87

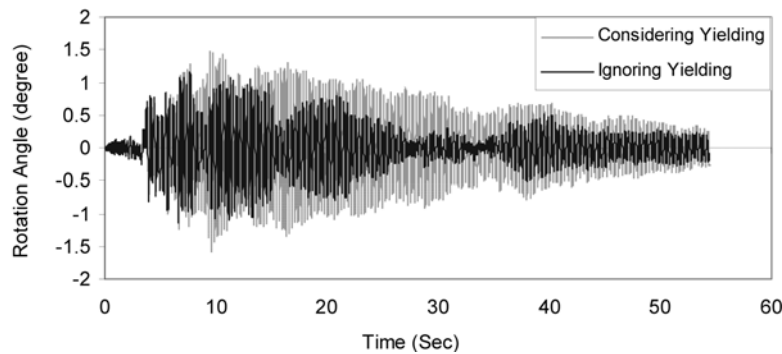


Fig. 8 Rotation angle of the 35 cm wall under Taft record, with and without considering the bar yielding, assuming that  $l = 20$  cm

### 6. Effect of separation length, $l$

In this section the influence of the separation length,  $l$ , on walls' seismic behavior is investigated. In this regard, the 35 cm thick wall (by the length and height of 4.5 and 3 m, respectively) is analyzed under Manjil, Tabas and Elcentro earthquake records, assuming  $l$  ranges of 2.5 to 22.5 cm; the results are shown in Fig. 9, 10 and 11 respectively. The results for Manjil earthquake are summarized in Table 6. As shown in the figures and table, the influence of the separation length on the rotation angle or maximum tensile forces of bars seems chaotic. In the literature of the deterministic physical and mathematical systems, chaotic is a term assigned to the motion classes with the time history of sensitive dependence on initial conditions (Moon 2004).

The chaotic behavior of the wall is confirmed by the results of similar analyses, for the 20 cm thick wall, under Manjil, Tabas and Elcentro earthquake records, shown in Fig. 12, 13 and 14, respectively. In both of the 20 or 35 cm thick walls, the variation procedures of the bar loads in earthquakes are similar; they all rise or drop together with respect to the separation length,  $l$ .

The relation between the rotation angles ( $\theta$ ) and maximum tensile forces of bars ( $F_1$ ,  $F_2$  and  $F_3$ ) is not practically linear. That is because of nonlinearities in the governing relation (Relation 19), as well as in the equivalent spring stiffness, bars behavior (regarding post yielding) and earthquake acceleration.

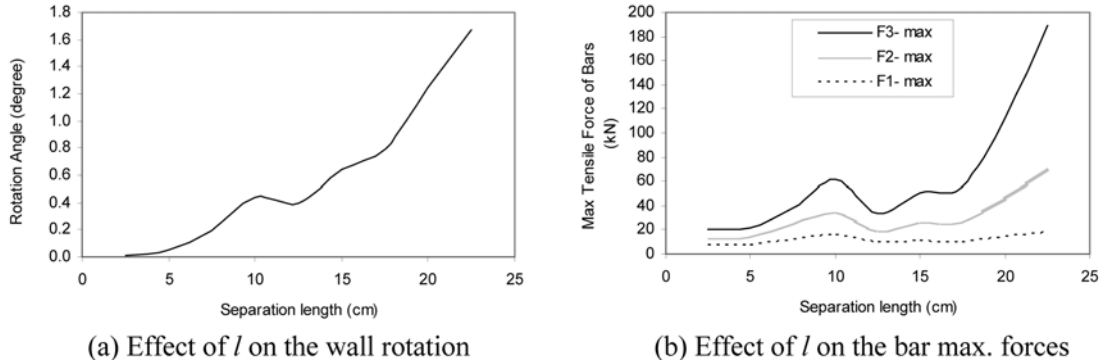


Fig. 9 Influence of the separation length on the seismic behavior of the 35 cm thick wall in Manjil earthquake

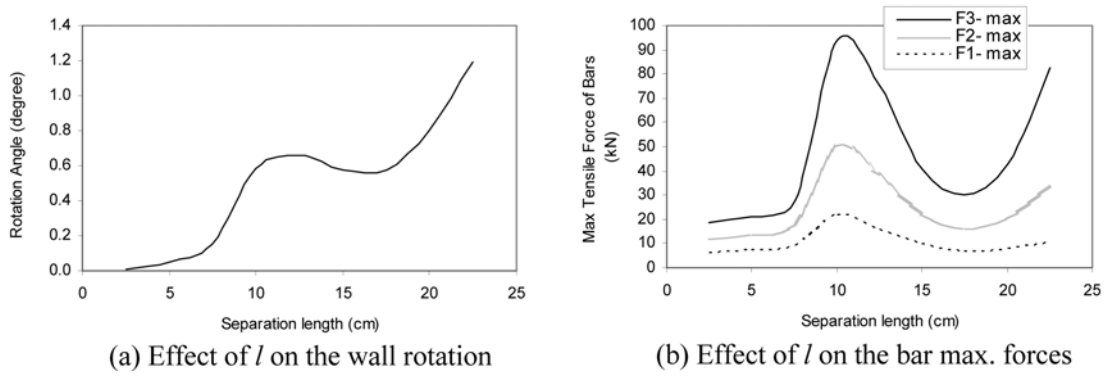


Fig. 10 Influence of the separation length on the seismic behavior of the 35 cm thick wall in Tabas earthquake

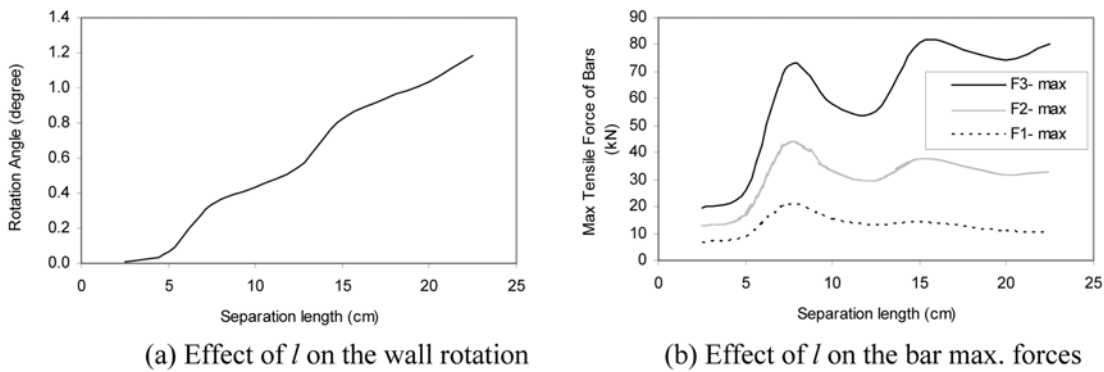
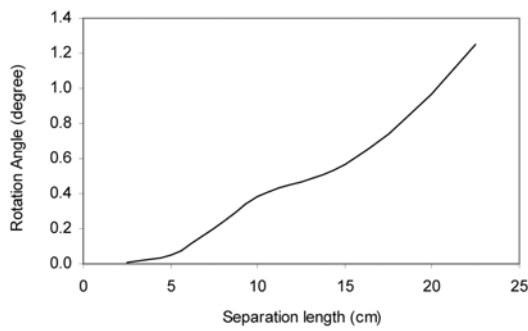


Fig. 11 Influence of the separation length on the seismic behavior of the 35 cm thick wall in Elcentro earthquake

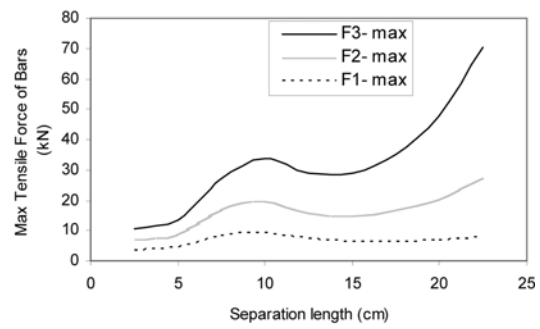
Furthermore, the ratio of F1 to F2 (or F3) is a function of the maximum wall rotation angle ( $\theta_{max}$ ) as shown in Table 7 for different separation lengths,  $l$ , in the 35 cm thick wall under Manjil earthquake. For very small  $\theta_{max}$ , the ratios depend directly on the bar height. Nevertheless, for high

Table 6 Influence of separation length,  $l$ , on the seismic behavior of the 35 cm thick wall in Manjil earthquake

Separation Length, $l$ (cm)	$\theta^+$ (deg)	$\theta^-$ (deg)	$F_3^+$ (kN)	$F_3^-$ (kN)	$F_2^+$ (kN)	$F_2^-$ (kN)	$F_1^+$ (kN)	$F_1^-$ (kN)
2.50	0.01	-0.01	20.00	-16.09	13.33	-10.72	6.66	-5.36
5.00	0.05	-0.04	22.12	-18.51	14.71	-12.32	7.34	-6.15
7.50	0.20	-0.16	38.62	-31.66	24.87	-20.59	12.17	-10.14
10.00	0.44	-0.36	60.96	-45.02	35.11	-27.07	15.86	-12.64
12.50	0.40	-0.38	33.65	-31.20	19.80	-18.55	9.10	-8.60
15.00	0.57	-0.65	40.14	-50.86	21.59	-26.20	9.22	-10.74
17.50	0.79	-0.78	55.08	-53.67	26.37	-25.81	10.01	-9.86
20.00	1.24	-1.23	113.64	-110.68	46.17	-45.13	13.86	-13.64
22.50	1.64	-1.67	179.58	-189.18	67.07	-70.32	16.89	-17.49

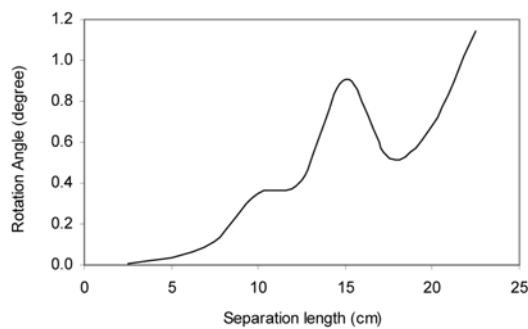


(a) Effect of  $l$  on the wall rotation

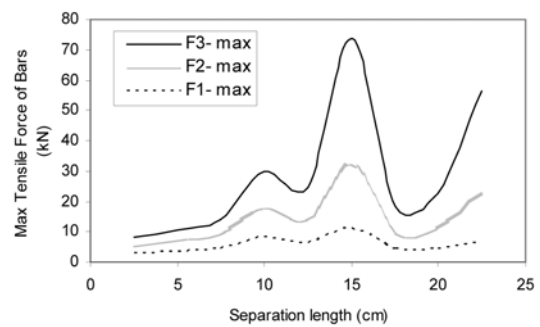


(b) Effect of  $l$  on the bar max. forces

Fig. 12 Influence of the separation length on the seismic behavior of the 20 cm thick wall in Manjil earthquake



(a) Effect of  $l$  on the wall rotation



(b) Effect of  $l$  on the bar max. forces

Fig. 13 Influence of the separation length on the seismic behavior of the 20 cm thick wall in Tabas earthquake

$\theta_{max}$ , maximum tensile force of the top bar rises much more rapidly than those of the bottom ones, shown in Fig. 15.

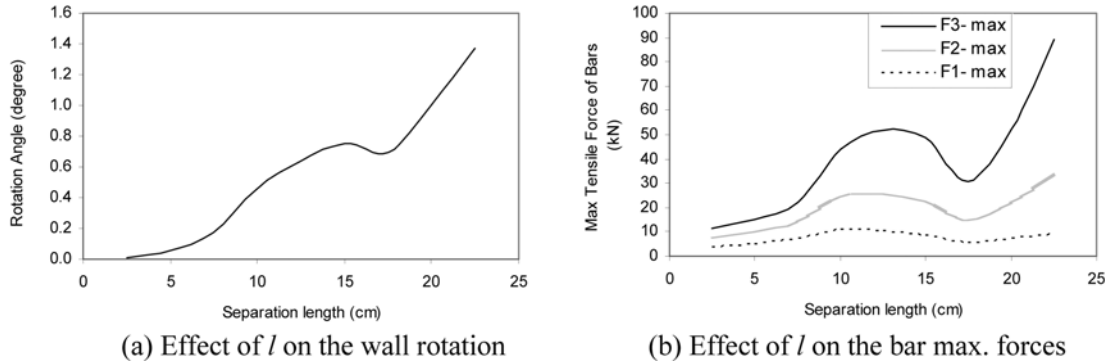


Fig. 14 Influence of the separation length on the seismic behavior of the 20 cm thick wall in Elcentro earthquake

Table 7 Maximum rotation of wall and ratio of the bars' tensile forces for the 35 cm thick wall in Manjil earthquake

$l$ (cm)	$\theta_{max}$ (degree)	F3/F2	F3/F1	F2/F1
2.5	0.01	1.50	3.00	2.00
5	0.05	1.50	3.01	2.00
7.5	0.20	1.55	3.17	2.04
10	0.44	1.74	3.84	2.21
12.5	0.40	1.70	3.70	2.18
15	0.65	1.94	4.74	2.44
17.5	0.79	2.09	5.50	2.63
20	1.24	2.46	8.20	3.33
22.5	1.67	2.69	10.82	4.02

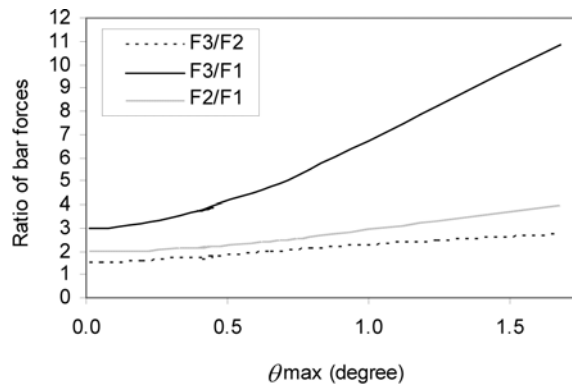


Fig. 15 Ratio of bar tensile forces with respect to the wall rotation, for 35 cm thick wall under Manjil earthquake record

## 7. Conclusions

Out of plane behavior of walls of normal sizes is investigated in this paper, based on the rigid block concepts. The walls are 3 m high, 4.5 m long, for which two thicknesses of 20 and 35 cm are considered. In this regard, reinforced bars that connect the wall to the adjacent elements-columns or perpendicular walls - are modeled as springs. The walls are analyzed for seven acceleration records, each in two cases: with natural PGA and normalized to 0.5 g. It is shown that the wall can be stabilized in out of plane direction during the assumed earthquakes by supplying some reinforcement. The required reinforcement is 3 $\Phi$ 18 and 3 $\Phi$ 20 for 20 cm and 35 cm thick wall, respectively, which are applied horizontally at the middle half of the wall by equal spacing. In necessities, the reinforcement can be replaced by equivalent bars of the same stiffness. Furthermore, a sensitivity analysis is performed for the influences of separation length,  $l$ . It is shown that influence of  $l$  is chaotic.

According to the results the wall rotation angle rises by regarding bar yielding. It is also shown that the maximum tensile forces of bars depend on a lot of parameters, including the bar situation and the higher bars has greater tensile forces.

## References

- Angle, R. and Abrams, D.P. (1994), "Out of plane strength of URM infill panels", NCEER-94-0004, 1-14.
- Dafnis, A., Kolsch, H. and Reimerdes, H.G. (2002), "Arching in masonry walls subjected to earthquake motions", *J. Struct. Eng-ASCE*, **128**(2), 153-159.
- De Felice, G. and Giannini, R. (2001), "Out of plane seismic resistance of masonry walls", *J. Earthq. Eng.*, **5**(2), 253-271.
- El-Dakhkhni, W.W., Hamid, A.A., Hakam, Z.H.R. and Elgaaly, M. (2006), "Hazard mitigation and strengthening of unreinforced masonry walls using composites", *Compos. Struct.*, **73**(4), 458-477.
- Fardis, M.N., Bousias, S.N., Franchioni, G. and Panagiotakos, T.B. (1999), "Seismic response and design of RC structures with plan-eccentric masonry infills", *Earthq. Eng. Struct. D.*, **28**, 173-191.
- FEMA 356 (2000), "Pre-standard for the seismic rehabilitation of buildings", Federal Emergency Management Agency, Second Draft.
- FEMA-273 (1997), "NEHRP Guidelines for the seismic rehabilitation of buildings, by the applied technology council (ATC-33 project)", Redwood city, CA, USA.
- Flanagan, R.D., Tenbus, M.A. and Bennett, R.M. (1994), "Numerical modelling of clay tile infills", NCEER-94-0004, 1-68.
- Housner, G.W. (1963), "The behavior of inverted pendulum structures during earthquakes", *B. Seismol. Soc. Am.*, **53**, 404-417.
- Jeong, M.Y. and Suzuki, K. (1997), "A study on the dynamic behavior of rocking rigid body using nonlinear rocking model", *Proceedings of the ASME Pressure Vessels and Piping Conferences*, Orlando, July.
- Makris, N. and Roussos, Y.S. (2000), "Rocking response of rigid blocks under near - Source ground motions", *Geotechnique*, **50**(3), 559-578.
- MATLAB-Matrix Laboratory (2006), Language of Technical Computing, Release R 2006 b, The MathWorks, Inc.
- Mendola, L.L., Papia, M. and Zingone, G. (1995), "Stability of masonry walls subjected to seismic transverse forces", *J. Struct. Eng-ASCE*, **121**(11).
- Moon, F.C. (2004), *Chaotic Vibrations, an Introduction for Applied Scientists and Engineers*, Wiley.
- Pena, F., Prieto, F., Lourenco, P.B., Campos Costa, A. and Lemos, J.V. (2007), "On the dynamics of rocking motion of single rigid-block structures", *Earthq. Eng. Struct. D.*, **36**(15), 2383-2399.

- Yim, C.S., Chopra, A.K. and Penzien, J. (1980), "Rocking response of rigid blocks to earthquakes", *Earthq. Eng. Struct. D.*, **8**(6), 565-587.
- Zang, J. and Makris, N. (2001), "Rockings response of free – standing blocks under cycloidal pulses", *J. Eng. Mech-ASCE*, 127(5).